How to cite: *Angew. Chem. Int. Ed.* **2024**, *63*, e202400815
doi.org/10.1002/anie.202400815

Radicals

# Reactivity of Superbasic Carbanions Generated via Reductive Radical-Polar Crossover in the Context of Photoredox Catalysis

*Sascha Grotjahn, Christina Graf, Jan Zelenka, Aryaman Pattanaik, Lea Müller, Roger Jan Kutta, Julia Rehbein, Jana Roithová, Ruth M. Gschwind, Patrick Nuernberger, and Burkhard König**

**Abstract:** Photocatalytic reactions involving a reductive radical-polar crossover (RRPCO) generate intermediates with carbanionic reactivity. Many of these proposed intermediates resemble highly reactive organometallic compounds. However, conditions of their formation are generally not tolerated by their isolated organometallic versions and often a different reactivity is observed. Our investigations on their nature and reactivity under commonly used photocatalytic conditions demonstrate that these intermediates are indeed best described as free, superbasic carbanions capable of deprotonating common polar solvents usually assumed to be inert such as acetonitrile, dimethylformamide, and dimethylsulfoxide. Their basicity not only towards solvents but also towards electrophiles, such as aldehydes, ketones, and esters, is comparable to the reactivity of isolated carbanions in the gas-phase. Previously unsuccessful transformations thought to result from a lack of reactivity are explained by their high reactivity towards the solvent and weakly acidic protons of reaction partners. An intuitive explanation for the mode of action of photocatalytically generated carbanions is provided, which enables methods to verify reaction mechanisms proposed to involve an RRPCO step and to identify the reasons for the limitations of current methods.

## Introduction

Within the last years, photocatalytic reactions involving a reductive radical-polar crossover (RRPCO)[1] step were reported by multiple groups. In an RRPCO a radical intermediate is converted to an anionic species, thus bringing the catalytic cycle back into the singlet spin-state while retaining reactivity for subsequent reaction steps. This allows the diversification of scaffolds obtainable by a single photocatalytic reaction. C-C bond formation through radical addition can be subsequently coupled to Grignard-type reactions,[2–5] rearrangements,[6] E1cB-type eliminations,[7] and intramolecular $S_N2$ reactions[8] as depicted in Scheme 1. Recently, reactions have been developed that focus especially on the generation of carbanions from easily accessible precursors such as decarboxylative carbanion generation[3] and C-H activation,[2,4,9–11] as well as carbanion generation from C-N[12] and C-O bonds,[13] to allow Grignard-type reactions, carboxylations, and isotopic labeling with up to 100 % atom economy. As RRPCO is a common step to close photocatalytic cycles, Scheme 1 provides only some selected examples. Other recent reactions proposed to proceed via an RRPCO step include photocatalytic dearomatizations,[14] Giese-type reactions,[15,16] and electrochemical cross-electrophile coupling.[17] Often the carbanionic intermediate is not explicitly mentioned if a catalytic cycle is closed by reduction of a radical species to a carbanion with subsequent protonation. These steps are then combined into a single reaction step described as electron transfer/proton transfer (ETPT) or as a stepwise proton-coupled electron transfer (PCET).

Despite the vast number of reactions achieved with classic organometallic carbanions such as Grignard[18] or organolithium reagents,[19] intermolecular C-C bond-forming reactions of photocatalytically generated carbanions seem to be restricted to carbon dioxide, aldehydes, and ketones with already noticeable drop in reaction yield from aldehydes to ketones.[2–4,9,10,16,20] Approaches to react carbanions generated

[*] S. Grotjahn, A. Pattanaik, L. Müller, Prof. Dr. J. Rehbein, Prof. Dr. R. M. Gschwind, Prof. Dr. B. König
Faculty of Chemistry and Pharmacy, Institute of Organic Chemistry
University of Regensburg
Universitätsstraße 31, 93053 Regensburg, Germany
E-mail: burkhard.koenig@ur.de

C. Graf, Dr. R. J. Kutta, Prof. Dr. P. Nuernberger
Faculty of Chemistry and Pharmacy, Institute of Physical and Theoretical Chemistry
University of Regensburg
Universitätsstraße 31, 93053 Regensburg, Germany

J. Zelenka, Prof. Dr. J. Roithová
Department of Spectroscopy and Catalysis
Radboud University Nijmegen
Heyendaalseweg 135, 6525AJ Nijmegen, the Netherlands

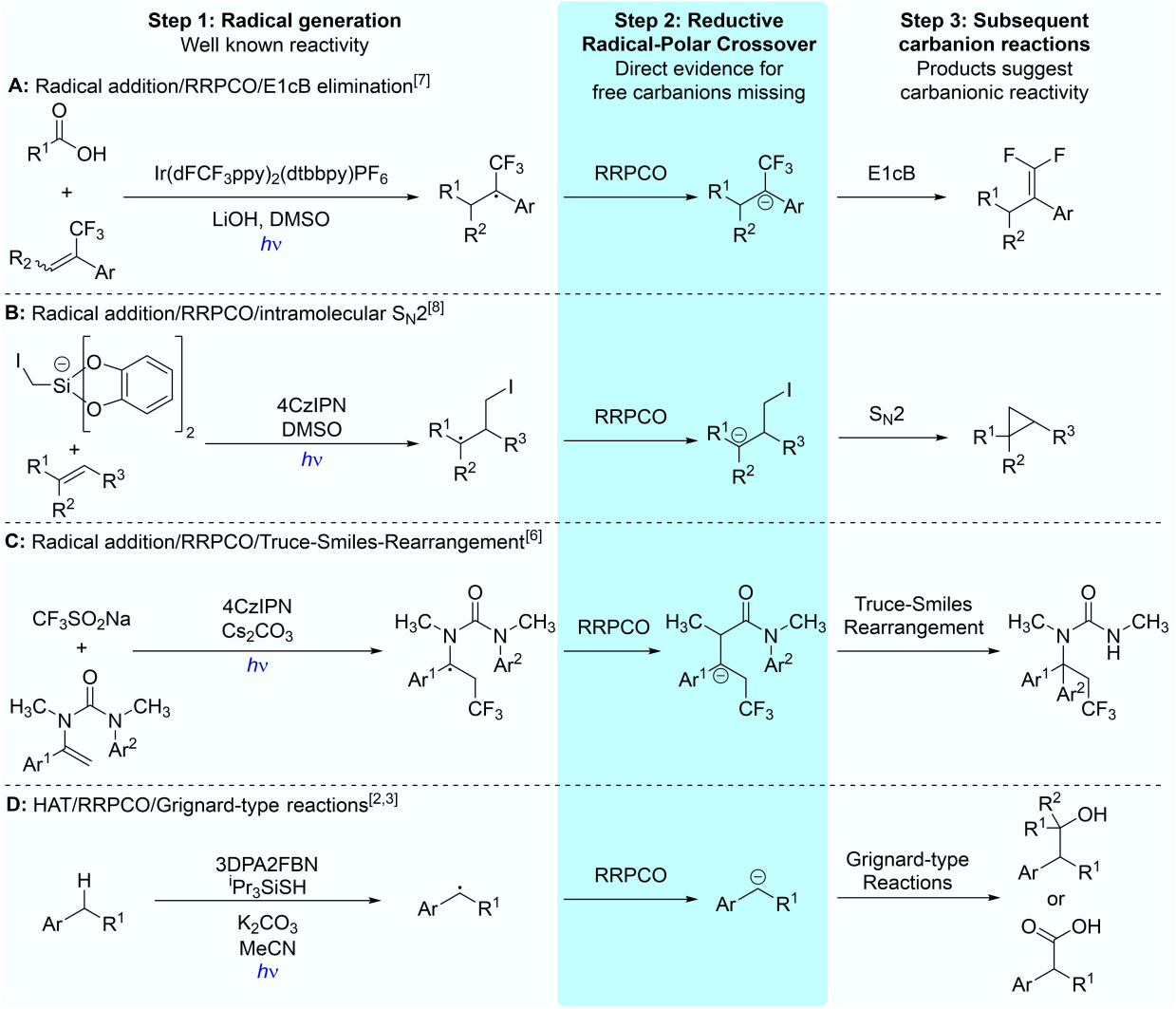


***Scheme 1.*** Selection of reactions proposed to involve a short-lived carbanionic intermediate. Abbreviation: RRPCO—reductive radical-polar crossover. HAT – Hydrogen Atom Transfer

under previously reported conditions in intermolecular $S_N2$ reactions or Grignard-type reactions with esters or similarly reactive electrophiles were generally unsuccessful. Here, we explore the nature of photocatalytically generated carbanions in more detail to give a rationale for the difference in reactivity compared to their organometallic analogs.

## Results and Discussion

### Evidence for Free Carbanions in Solution

The reports on reactions involving photocatalytically generated carbanions depicted in Scheme 1 provide clear evidence for carbanionic reactivity. The usual control reaction for distinguishing between a radical pathway and carbanionic reactivity is the addition of $D_2O$ to the reaction mixture, quenching the carbanion and incorporating deuterium at the respective position. Although this experiment provides evidence for carbanionic reactivity and generally excludes a direct radical pathway, it does not provide information about whether the carbanion is truly a free carbanion or stabilized by some kind of interaction with a species present in the reaction mixture. Even classical organometallic reagents show a pronounced difference in reactivity for different alkali and alkaline earth metal compounds due to aggregation and ion pairing.[21] However, a direct comparison of the reactivity in the same environment with organometallic reagents is not possible due to the incompatibility of highly reactive organometallic compounds with solvents generally used in photocatalytic reactions generating carbanions. This incompatibility of classic organometallic reagents with high polarity solvents raised the question why photocatalytic reactions proposed to involve a carbanion were possible under these conditions. We found that under absence of a suitable coupling partner for carbanions the corresponding protonated species is formed as the major product. When using $CD_3CN$ as solvent a high

degree of deuteration at the benzylic position can be obtained, depending on the electronic properties of the carbanion formed, thus demonstrating that the solvent indeed cannot be assumed to be inert. The addition of $H_2O$ suppresses this deuteration while addition of $D_2O$ leads to high deuteration even in non-deuterated solvents. The degrees of deuteration for a selection of electronically different substrates is depicted in Scheme 2. $d_x$ describes the number of deuterium atoms in the molecule, with the non-deuterated molecule labelled with $d_0$. A more detailed description on the determination of deuteration degrees can be found in the Supporting Information section 7.

The deprotonation of the only slightly acidic acetonitrile C-H bonds (or C–D bonds) with a p$K_a$ of approximately 31

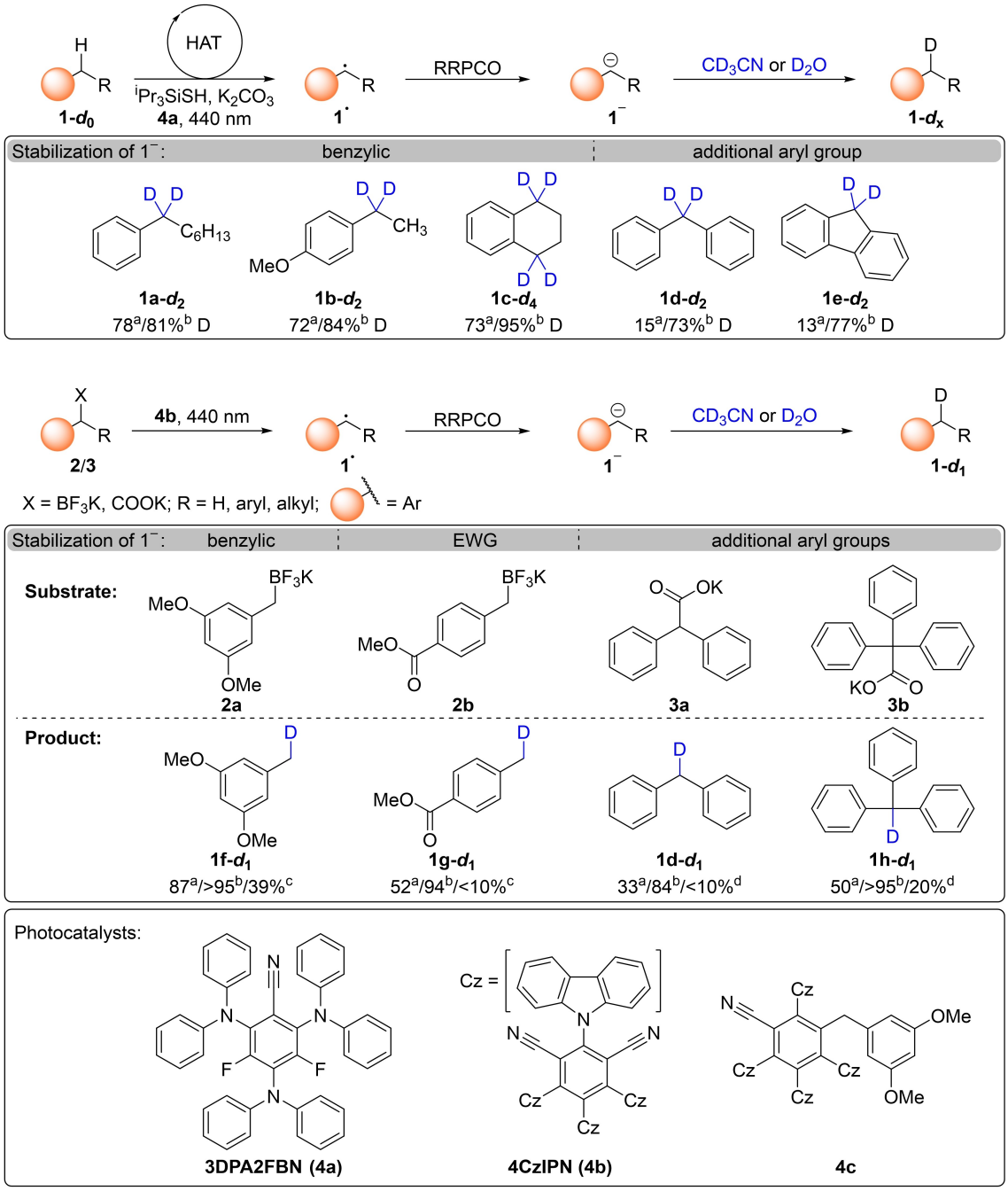


***Scheme 2.*** Deuterium incorporation into the benzylic position. Deuteration degrees are determined by $^1$H NMR spectroscopy and based on the theoretically possible equivalents of deuterium that can be incorporated based on the mechanism (1 D per benzylic hydrogen of the substrate [2 D per molecule] in C-H activation, 1 D per molecule in carbanion generation from trifluoroborates and carboxylates); photocatalyst **4c** is formed in situ from 4CzIPN (**4b**) and trifluoroborate **2a**;[22] [a]deuteration without $D_2O$; [b]deuteration with 10 equiv. $D_2O$; [c]0.5 equiv. of $H_2O$ added to provide 1 equiv. of protons; [d]carboxylic acid with 1 equiv. $Cs_2CO_3$ used instead of potassium salt, no $D_2O$ was added. RRPCO – reductive radical polar crossover; HAT – hydrogen atom transfer; EWG – electron withdrawing group

(dissolved in DMSO)[23] by non-stabilized benzylic carbanions **1a**$^-$, **1b**$^-$, **1c**$^-$, and **1f**$^-$ demonstrates that photocatalytically generated carbanions can be highly basic. It was expected that compounds with higher C-H acidity would generate less basic carbanions upon C-H activation. Indeed, benzylic C-H activation of diphenylmethane (**1d**) and fluorene (**1e**) to the corresponding carbanions **1d**$^-$ and **1e**$^-$, respectively, was achieved under standard reaction conditions but only low D-incorporation was observed in dry $CD_3CN$, while deuteration was high in the presence of 10 equivalents $D_2O$. Carbanions generated from carboxylates and trifluoroborate salts follow the same trend with high incorporation of deuterium into non-stabilized benzylic carbanion **1f**$^-$ and decreasing D-incorporation with better stabilization of the negative charge, while D-incorporation remains high in all examples in the presence of $D_2O$. For less reactive carbanions stabilized by electron withdrawing groups (**1g**$^-$) or an additional aryl group (**1d**$^-$, **1e**$^-$, **1h**$^-$) under proton free conditions there is still moderate deuterium incorporation into the product. However, the lack of abstractable protons likely leads to regeneration of the starting material by reaction of the carbanion with the formed $CO_2$ or $BF_3$ which can then re-enter the photocatalytic cycle until either a deuteron is abstracted from $CD_3CN$ or a proton from another source (e.g., residual moisture). The reaction of carbanions generated under similar conditions with $CO_2$ was reported previously[9] and is also observed in the gas phase (see SI, Figure S13). More comparable results are obtained if one equivalent of abstractable protons is still present in the reaction mixture. For carbanion generation from carboxylates this is achieved by using the carboxylic acid and a mild base instead of a carboxylate salt, which resembles a previously described procedure for photocatalytic Grignard-type reactions.[3] For trifluoroborates (**2**), 0.5 equivalents of water were added to provide 1 equivalent of protons. If carbanions are generated from C-H bonds the abstracted hydrogen atoms remain in solution as hydrogen carbonate and silane thiol, thus a small amount of acidic protons is always present under these conditions. Proton (or deuteron) abstraction from the solvent by stabilized carbanions **1g**$^-$, **1d**$^-$, and **1h**$^-$ is mostly suppressed if acidic protons are present, while non-stabilized carbanions are less selective and abstract protons (or deuterons) from the solvent even in presence of substantially more acidic protons. The difference in reactivity of non-stabilized and stabilized carbanions towards moderately acidic protons has important synthetic implications for isotopic labelling, especially for tritium labelling where it is desirable to quantitatively incorporate tritium from stoichiometric amounts of the tritium source into a target molecule to minimize radioactive waste.[24] Deprotonation of the solvent also occurs in DMSO, DMF, and acetone. Potassium trifluoroborate salt **2a** was used as carbanion precursor because trifluoroborates generate carbanions more reliably under different reaction conditions, while carbanion generation from carboxylates is more sensitive to the reaction conditions. In DMSO-$d_6$ as well as in acetone-$d_6$ the corresponding 3,5-dimethoxytoluene (**1f-$d_1$**) was produced with high degree of mono-deuteration, similar to the outcome in acetonitrile-$d_3$ (Scheme 3) and in DMF-$d_7$ a moderate deuteration degree of 42 % was observed. In acetone the corresponding tertiary alcohol **7b** was obtained in similar amounts as the toluene derivative **1f-$d_1$**, (Scheme 8, see below). Deprotonation of the solvent generates the corresponding solvent anion **5**$^-$. We could indirectly detect this species formed from acetonitrile-$d_0$ in the presence of 1 equivalent $D_2O$. Under these reaction conditions the deprotonated solvent was deuterated by $D_2O$ to form acetonitrile-$d_1$ which was detected in the $^2$H NMR spectrum (see SI, Figure S31).

### *Comparison with Gas-Phase Reactivity of Isolated Carbanions*

Next the reactivity of isolated/non-solvated carbanions generated via collision-induced dissociation (CID) was tested in the gas phase (Figure 1, see Supporting Information section 6 for details). In agreement with the results obtained under photocatalytic conditions in solution, non-stabilized benzylic carbanions readily deprotonate α-positions of carbonyl and nitrile groups. Carbanions with additional stabilization by an electron withdrawing ester group

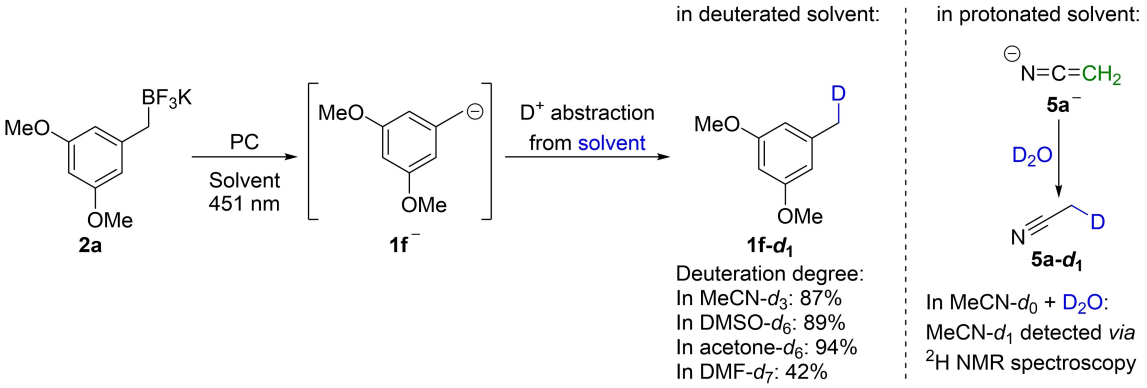


***Scheme 3.*** Photocatalytically generated non-stabilized benzylic carbanion **1f**$^-$ is able to abstract a deuteron from acetonitrile-$d_3$, DMSO-$d_6$, DMF-$d_7$, and acetone-$d_6$. MeCN-$d_1$ was detected by deuterium NMR spectroscopy when the reaction was performed in acetonitrile-$d_0$ in the presence of $D_2O$. PC—photocatalyst **4c** is generated in situ from 4CzIPN (**4b**).[22]

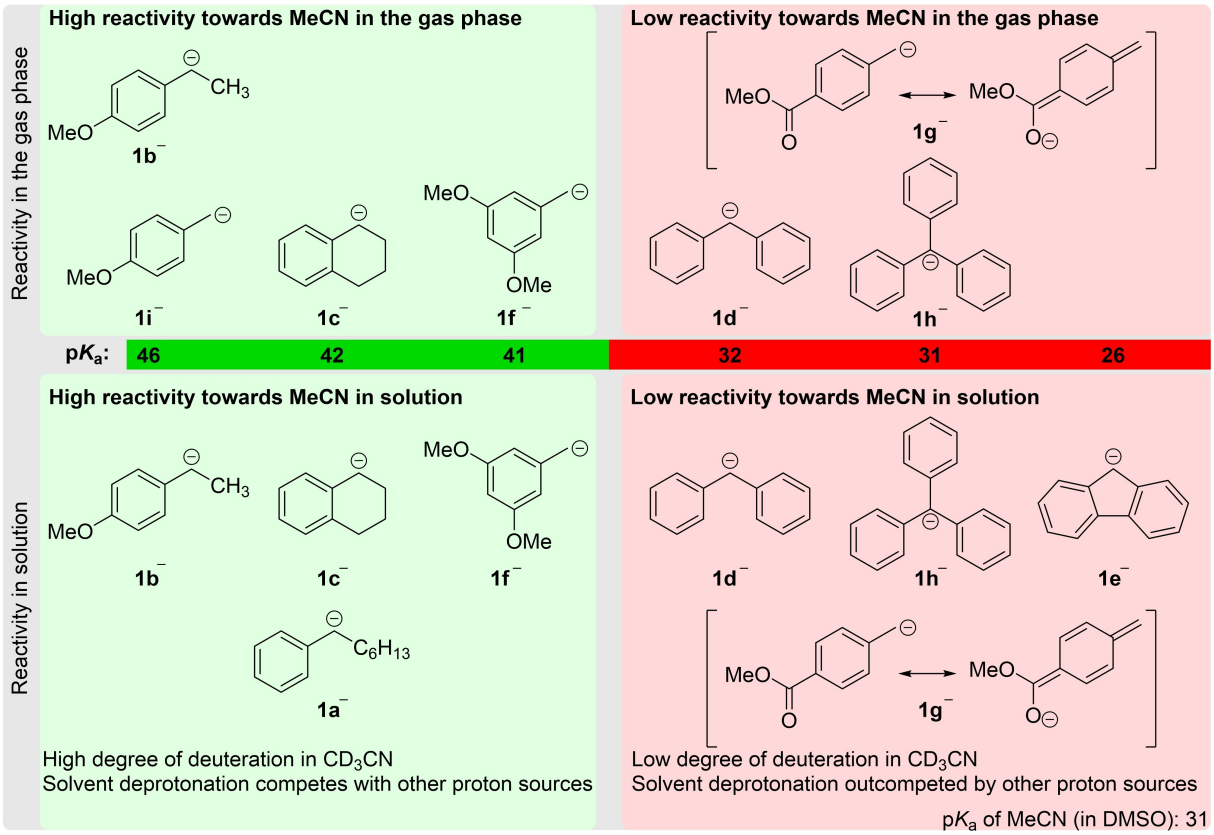


***Figure 1.*** Gas phase reactivity of carbanions generated via collision-induced dissociation (CID) with acetonitrile, and comparison with its solution reactivity. Molecules are grouped into high reactivity towards deprotonation of MeCN and low or no reactivity towards MeCN. Molecules are placed at the approximate p$K_a$ values of the respective conjugate acid, where values of the respective compound or closely related compounds in DMSO are accessible.[23,25,26]

(**1g**$^-$) on the aryl group or additional phenyl groups (**1d**$^-$, **1e**$^-$, **1h**$^-$) at the benzylic position did not deprotonate acetonitrile in the gas phase. A strong drop in reactivity under the photocatalytic conditions used to generate carbanions in solution was also observed for all carbanions with conjugated acids with a p$K_a$ close to or below that of acetonitrile. Thus, basicity of carbanions generated under photocatalytic conditions relative to acetonitrile is similar to isolated carbanions in the gas phase.

In addition to qualitatively separating carbanions into high and low reactivity towards acetonitrile, the deprotonation in the gas phase showed a pronounced kinetic isotope effect (KIE). Following KIEs for reactions with acetonitrile-$d_0/d_3$ were found: for anion **1f**$^-$ 6.5±0.5, for **1b**$^-$ 3.2±0.5, for **1i**$^-$ 3.0±1.0 and for **1c**$^-$ 4.0±0.5, in agreement with their relative p$K_a$ difference to acetonitrile.[27] The same experiment with photocatalytically generated carbanion **1f**$^-$ in solution with varying mixtures of acetonitrile-$d_0/d_3$ resulted in a KIE of 9.0. The theoretical KIE calculated at the B97D3/Def2TZVP level of theory is 6.8 and, thus, in line with the experimental values of 6.5 in the gas-phase and 9.0 in solution. Although exact p$K_a$ values cannot be derived solely from KIE data and vice versa, the experimental results of gas phase and solution KIEs are in the range expected according to the Bell-Goodall curve revised by Bordwell and Boyle.[27] Extensive studies on proton transfer KIEs with photocatalytically generated carbanions are outside the scope of this work but the results suggest that the obtained KIEs are suitable for experimental estimation of the basicity of carbanionic intermediates, which are too basic to be stable in the respective solvent.

### *Isotopic Fractionation and Kinetic Isotope Effects*

Recently, an isotopic fractionation method was described for determining the sequence of elementary steps in hydrogen isotope exchange (HIE) reactions based on the observation that hydrogen atom abstraction usually has a larger KIE than deprotonation.[28] If an HIE reaction proceeds via a reversible hydrogen atom transfer (HAT), the H-atom abstraction and donation proceed via the same transition state and, thus, have the same KIE. As the KIEs of both steps influence the equilibrium D/H fraction in opposing directions the D/H fraction is solely dependent on the equilibrium D/H fraction of the HAT reagent, which usually does not show a strong isotope effect. Therefore, a direct linear correlation between the equilibrium D/H ratio and the D/H ratio of a D/H reservoir is expected. A slope

substantially deviating from 1 indicates that H-atom abstraction and donation proceed via distinct transition states.

We applied this concept to the carbanion generation from benzylic C-H bonds on the example of ethyl anisole (**1b**), in which the reaction does not reach its equilibrium state. Correlating the product D/H ratio with the isotopic fractionation from partially deuterated starting material resulted in a slope of ca. 8.5, which is in agreement with the value of 7.2 expected from the individual steps as determined according to Scheme 4. Indeed, a slightly higher experimental D/H ratio than calculated from the individual steps is expected due to secondary KIEs. Abstraction of an H-atom from **1b-$d_0$** is favored over abstraction of an H-atom from **1b-$d_1$**, while abstraction of a D-atom from **1b-$d_1$** is favored over abstraction of a D-atom from **1b-$d_2$**, thus, shifting the equilibrium D/H ratio further to the side of deuterium. Moreover, the result of an H/D ratio clearly above 1.5 is in agreement with the proposed mechanism of an HAT followed by an electron-transfer, proton-transfer (ETPT) sequence. This demonstrates that the isotopic fractionation method is not only applicable to reactions reaching equilibrium, but also enables approximate values for lower catalyst turnovers.

The KIE of the HAT-step was determined from the coupling between ethyl anisole mono-deuterated at the benzylic position (**1b-$d_1$**) and benzophenone **6** as coupling partner because **6** can react in a radical-radical recombination with benzylic radical **1b**° generated via HAT but can also react with carbanion **1b**$^-$ formed upon reduction of the radical **1b**°.[29] Since the reduction potentials for both, radical **1b**° and benzophenone **6** are −1.8 V vs. SCE,[25,30] they can be reduced to the corresponding carbanion and radical anion, respectively, by the photocatalyst 3DPA2FBN (**4a**) with a reduction potential of −1.9 V vs. SCE.[31] Trapping carbanions by aldehydes or ketones with α-C-H bonds could give misleading results due to deprotonation in α-position (Schemes 7 and 8) of the carbonyl reaction partner. Additionally, protons from the solvent and residual water can be incorporated into the substrate, if carbanions are generated preferentially, potentially leading to scrambling of the deuterium between substrate molecules and D-H exchange between substrate and solvent, which should be minimized to reduce the experimental error.

### *Excited State Dynamics of 4d in the Absence and Presence of 2a and the Role of Molecular Oxygen*

Transient absorption (TA) spectroscopy was used to observe short-lived intermediates. Although carbanion **1f**$^-$ generated under photocatalytic conditions could not be directly observed, the timescales of the individual processes were estimated by following the transient species of photocatalyst **4d**. Recording the transient absorption of photocatalyst **4d** excited at 355 nm under ambient conditions (ca. 23 °C) in acetonitrile, a broad positive absorption of the triplet state $^3$[**4d**] ranging from ca. 300 to 750 nm is observed within the temporal width of the excitation pulse, intersected by a strong negative emission from the first excited singlet state $^1$[**4d***] peaking at 500 nm and a negative ground state bleach (GSB) peaking at ca. 375 nm (Figure S46). While the short emission signal decays within the temporal width of the excitation pulse, the triplet absorption and GSB signals exhibit a decay on a 1 µs time scale indicative of reverse

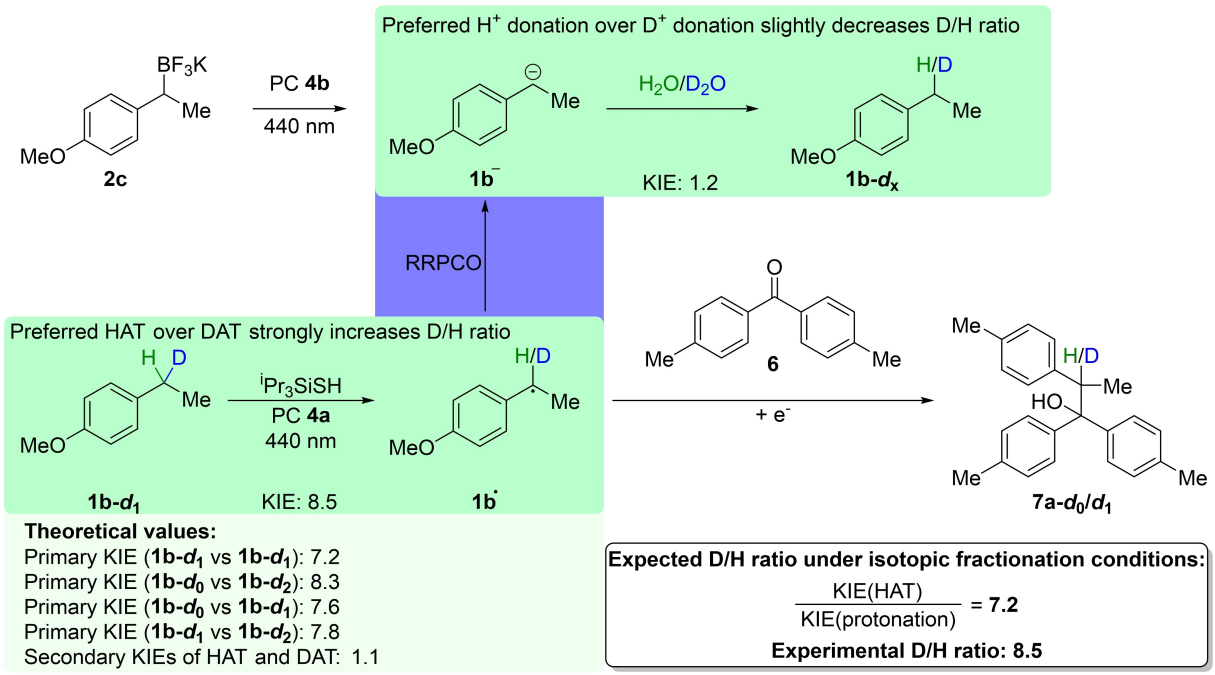


***Scheme 4.*** Kinetic isotope effects for HAT and protonation measured independently. If carbanions are generated via C-H activation both steps are connected via a RRPCO step. PC—Photocatalyst **4b** was used as pre-catalyst. The active catalyst was formed *in-situ* via photosubstitution.[22]

intersystem crossing into the ground-state species without formation of further intermediates and photoproducts, rendering **4d** as a photostable compound, which is also evident from the steady-state absorption prior and post the TA recording (Figure S47). Time-resolved emission studies of $^{1}$[**4d***] disclose an excited-state lifetime of 18 ns (Figure S48a) that is not resolved in the TA data. The $^{3}$[**4d**] spectrum (Figure S49a) decays under non-degassed conditions with a lifetime of 453 ns, in agreement with thermally activated delayed fluorescence (TADF) decaying on the order of 400 ns (Figure S48a).

After removing molecular oxygen from the solution, the lifetime of $^{1}$[**4d***] is prolonged to 28 ns (Figure S48b). In the TA data, identical spectral features are observed, but the triplet lifetime is prolonged to 19.7 µs, demonstrating that the triplet $^{3}$[**4d**] undergoes a diffusion-controlled reaction with molecular oxygen via energy transfer. Considering a concentration of molecular oxygen of $c(O_2) = 2.42$ mM,[32] the bimolecular rate constant is given to $k_{O_2} = \frac{k_{T1} - k_{T1}^{-O2}}{c(O2)} = 8.91 \cdot 10^8\ M^{-1}s^{-1}$ ($k_{T1}$ and $k_{T1}^{-O2}$ are the rate constants in the presence and absence of $O_2$, respectively), which is close to the diffusion limit.

In the presence of the substrate **2a** (10 mM, which is close to the solubility limit) under non-degassed conditions, no further spectra of species other than the triplet state become obvious. However, the triplet state lifetime is quenched to 397 ns indicating an additional reaction with a yield of $1 - k_{T1}/k_{T1}^{2a} = 12.6\,\%$ ($k_{T1}$ and $k_{T1}^{2a}$ are the rate constants in the presence and absence of **2a**, respectively). Thus, the formed reaction products either do not absorb in the experimental spectral detection window or molecular oxygen reacts faster with these intermediates forming new species which also do not absorb significantly in the accessible spectral range. Comparing the steady-state absorption spectra before and after the TA recordings, a new absorption contribution is evident, which confirms photoproduct formation (Figure S47).

In the presence of **2a** (10 mM) but in the absence of $O_2$ the intrinsic lifetime of $^{3}$[**4d**] is quenched from 19.7 µs to 5.0 µs and the decay of the triplet spectrum is accompanied by the rise of new spectral contributions that persist on a time scale longer than 1 ms (Figure 2). As the persisting difference spectrum is in striking agreement with the difference spectrum of the electrochemically formed radical anion of **4d**$^{\circ-}$ and its ground-state absorption (Figure S50a), the newly formed species arises from a diffusion-controlled electron transfer from **2a** to the triplet $^{3}$[**4d**], which in the absence of molecular oxygen becomes highly efficient with $1 - k_{T1}^{-O2}/k_{T1}^{2a,-O2} = 74.6\,\%$ ($k_{T1}^{-O2}$ and $k_{T1}^{2a,-O2}$ are the rate constants in the presence and absence of **2a** under degassed conditions, respectively) of the $^{3}$[**4d**] molecules being quenched in this way. With a maximum **2a** concentration of $c(\mathbf{2a}) = 10$ mM, the bimolecular rate constant is given to $k_{2a} = \frac{k_{T1}^{2a,-O2} - k_{T1}^{-O2}}{c(2a)} = 1.49 \cdot 10^7\ M^{-1}s^{-1}$ ($k_{T1}$ and $k_{T1}^{-O2}$ are the rate constants in the presence and absence of $O_2$, respectively). Since on this time scale the reaction with residual $O_2$ is negligible, **4d**$^{\circ-}$ can accumulate under these conditions. The

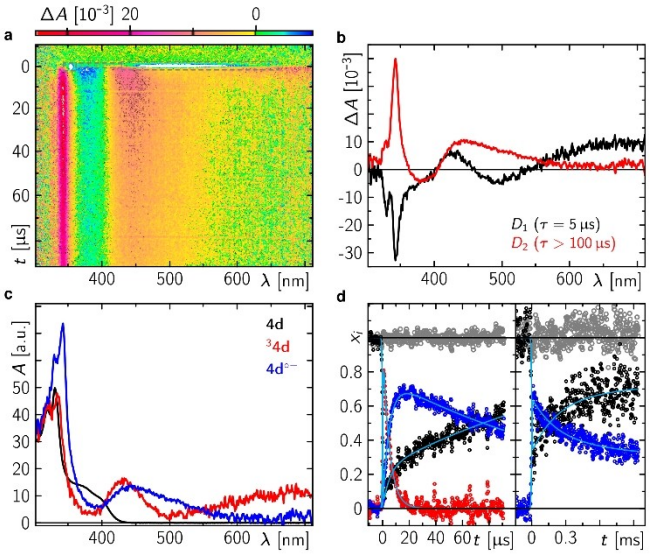


***Figure 2.*** Time-resolved absorption data of **4d** in the presence of **2a** (10 mM) and absence of $O_2$ following excitation at 355 nm. (**a**) Time-resolved spectra. The dashed rectangles indicate data ranges that were excluded from the global analysis as described elsewhere.[33] (**b**) decay associated difference spectra as a result from a global bi-exponential fit to the data in (**a**). (**c**) Species associated spectra (SAS) contributing to the data in (**a**) as indicated. (**d**) Mole fraction-time profiles of the SAS (open circles) contributing to the data in (**a**) and to data recorded in a 1 ms time window (Figure S46). The corresponding global fits are shown as cyan lines.

decay of **4d**$^{\circ-}$ can be well described by a bi-exponential ansatz with lifetimes of 231 µs and ≫1 ms (Figure 2). As the **4d**$^{\circ-}$ formation is accompanied by **2a**$^{\circ}$ and subsequent **1f**$^{\circ}$ formation to the identical amount the first phase of the **4d**$^{\circ-}$ decay may be attributed to RRPCO forming the carbanion **1f**$^{-}$ and partially the initial **4d** (Scheme 5) while residual radicals **1f**$^{\circ}$ undergo dimerization to bibenzyl **8a**, leaving some **4d**$^{\circ-}$ after consumption of all benzyl radicals. Since all reactive intermediates **1f**$^{\circ}$ have either dimerized or undergone electron transfer within 500 µs, the second phase of the **4d**$^{\circ-}$ decay may result from reaction with residual $O_2$ forming a new photoproduct.

As the steady-state absorption spectra after the TA recording of the degassed samples in the presence and absence of **2a** differ (Figure S47), it is tempting that the latter scenario plays a significant role. Since neither spectral features of **1f**$^{\circ}$ nor of **1f**$^{-}$ are observed, their lifetimes may only be estimated based on the dynamics of the accompanying counter radical **4d**$^{\circ-}$. As the **4d**$^{\circ-}$ dynamics is biphasic, dimerization and RRPCO compete on the time scale of the first phase of the **4d**$^{\circ-}$ decay. Since nucleophilic additions to aliphatic aldehydes[3] could be detected in a preparative ansatz, only accessible via bimolecular reactions, this requires a lifetime of the carbanion on the diffusion time scale of µs at substrate concentrations in the mM range in solvents with similar viscosities as acetonitrile.

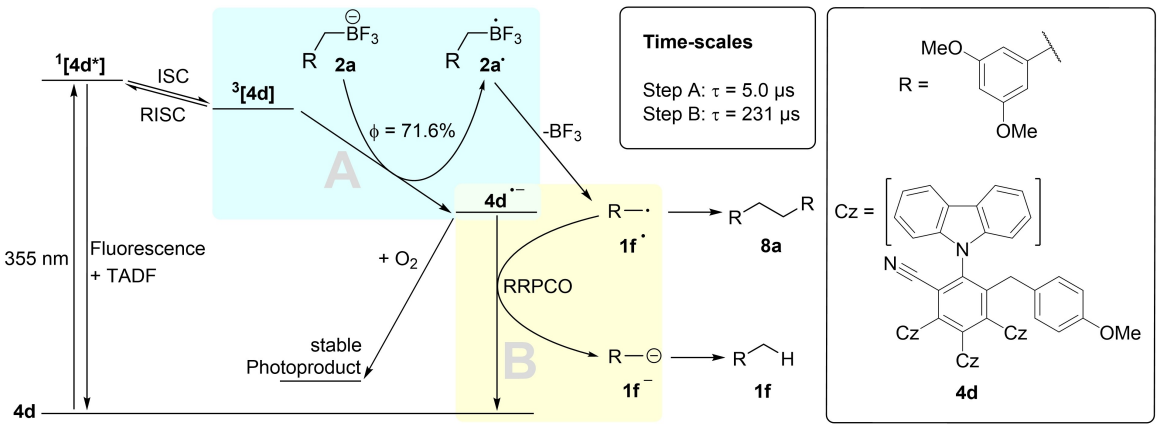


***Scheme 5.*** Proposed photocatalytic cycle for dimerization and carbanion formation from **1f**° mediated by triplet $^3$[**4d**] in ACN. **4d** is excited into the singlet state $^1$[**4d***], which then either fluoresces or undergoes intersystem crossing (ISC) and reaches the triplet state $^3$[**4d**]. Reverse intersystem crossing (RISC) partially occurs, leading to thermally activated delayed fluorescence (TADF). Initial electron transfer from **2a** to $^3$[**4d**] forms a radical pair $^3$[**4d**$^{\circ-}$,**1f**°] that partially proceeds via RRPCO regenerating the **4d** and forming the carbanion **1f**$^-$, which deprotonates ACN. Dimerization of **1f**° significantly reduces carbanion formation, so that **4d**$^{\circ-}$ partly reacts with residual oxygen. Both products could be identified by mass analysis (Figure S51 and S52).

### *Importance for Reactions Involving Photocatalytically Generated Carbanions*

The high basicity of photocatalytically generated carbanions poses important consequences and limitations for their utilization in organic synthesis. Standard solvents used in photoredox catalysis such as MeCN and DMSO possess weakly acidic protons that can be abstracted by highly basic carbanions formed under photocatalytic RRPCO conditions. Intermolecular C-C bond-forming reactions usually cannot compete with a fast deprotonation of the surrounding bulk solvent unless the reaction partner is sufficiently electrophilic. An intramolecular example is the photocatalytic C-H activation of phenylvaleric acid ethyl esters to the corresponding carbanions[2] where solvent reactivity is expected to be the limiting parameter. When such cyclizations are conducted in acetonitrile-$d_3$ the recovered starting material has a high degree of deuteration at the benzylic position. In agreement with a direct competition between intramolecular Grignard reaction and solvent deprotonation, the increase in steric bulk on the ester leads to a decrease in yield of cyclization product, while the degree of deuteration at the benzylic position increases (Scheme 6). These findings demonstrate that formation of cyclization product 2-phenylcyclopentanone (**10**) is primarily limited by the rate constant of carbanion protonation relative to cyclization.

In contrast to phenylvaleric acid ethyl ester (**9b**), the homolog which is shorter by one methylene group, phenylbutyric acid ethyl ester, did not cyclize to the corresponding 2-cyclobutanone and the longer phenylhexanoic acid ethyl ester did only give traces of the corresponding 2-phenylcyclohexanone (**12**).[2] While a four-membered ring is expected to be thermodynamically unfavorable, formation of 2-phenylcyclohexanone (**10**) from 6-phenylhexanoic acid ester **9** should be energetically more favorable compared to cyclization of the corresponding phenylvaleric acid ester **7a** to phenylcyclopentanone **8**. Subjecting deuterated phenylhexanoic acid ester **11-C2-$d_2$** to the conditions for benzylic carbanion generation according to Scheme 7, no shift of deuterium from the α-position of the ester to the benzylic position was observed and the deuteration degree of the starting material at C2 remained unchanged, thus excluding an intramolecular deprotonation. Conducting the reaction in $CD_3CN$ gave additional 71 % deuteration at the benzylic position. The analogous reaction with deuterated phenylvaleric acid ester **9a-C2-$d_2$** confirmed no intramolecular deuterium transfer also for the shorter homolog. This is in agreement with literature reports corroborating that activation barriers for proton transfer reactions increase with deviation from a linear transition state.[34]

The barriers for cyclization of the carbanions derived from phenylvaleric acid methyl ester (**9a**) and phenylhexanoic acid methyl ester (**11**) calculated at the M06-2X/6-31G(d) level of theory for optimization and frequency analysis and at the wB97XD/Def2TZVP level of theory for single point are 5.9 kcal/mol and 2.1 kcal/mol, respectively, and thus are contrary to the experimental trend. This suggests the relative rates of cyclization are primarily influenced by diffusional motion between the reacting moieties. While the rate for carbanion protonation by the solvent is expected to be independent of the alkyl chain length, cyclization will proceed faster for shorter chains due to significantly shorter average distances between the benzylic position and the carbonyl group as well as due to less sampled configurational space during diffusion.

The strong basicity of photocatalytically generated benzylic carbanions is not only relevant with respect to the solvent but also towards reaction partners with weakly acidic protons such as acetone, a common reaction partner for Grignard-type reactions, having mildly acidic α-protons and being readily available in its deuterated form. Indeed, when generating carbanion **1f**$^-$ in acetone-$d_6$ according to Scheme 8, the corresponding mono-deuterated toluene derivative **1f-$d_1$** and the addition product **7b** were obtained in

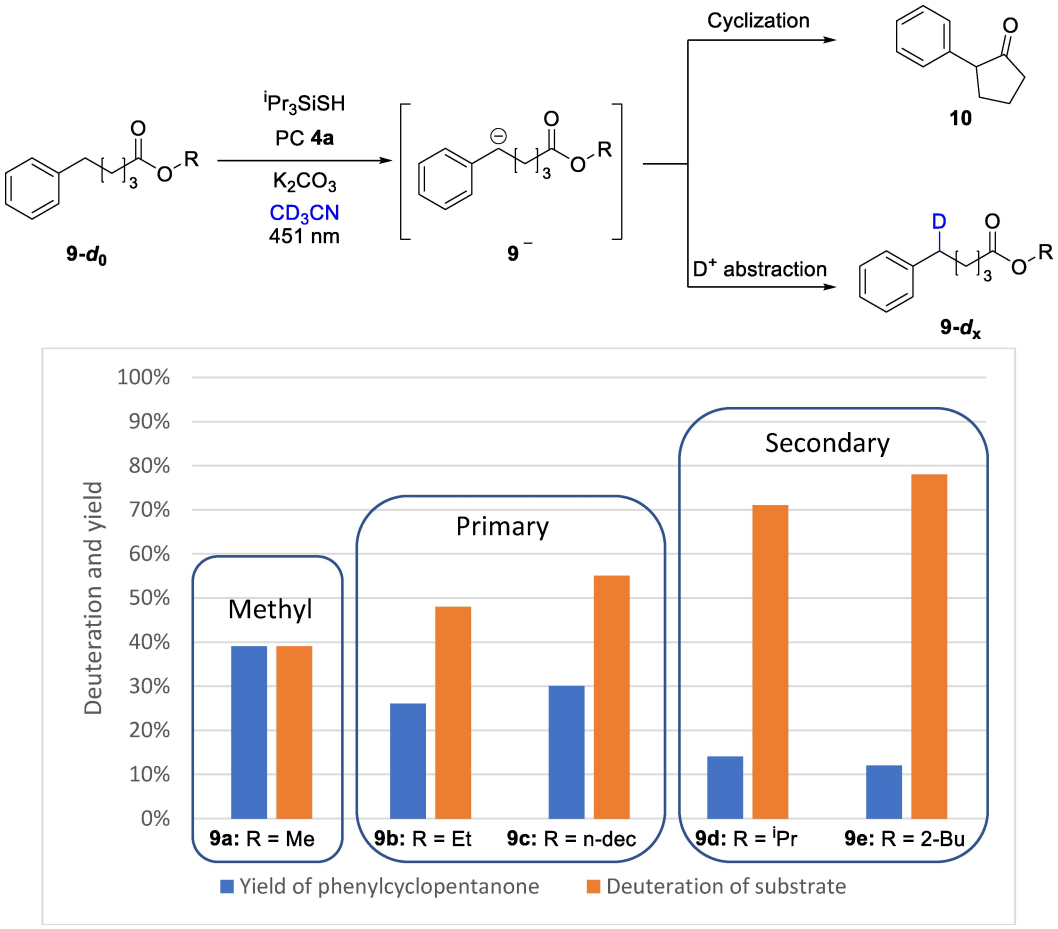


***Scheme 6.*** 5-Phenylvaleric acid esters **9a–e** cyclize to 2-phenylcyclopentanone (**10**). Solvent deprotonation competes with Grignard-type cyclization. Yield and degree of deuteration determined by $^{1}$H NMR spectroscopy.

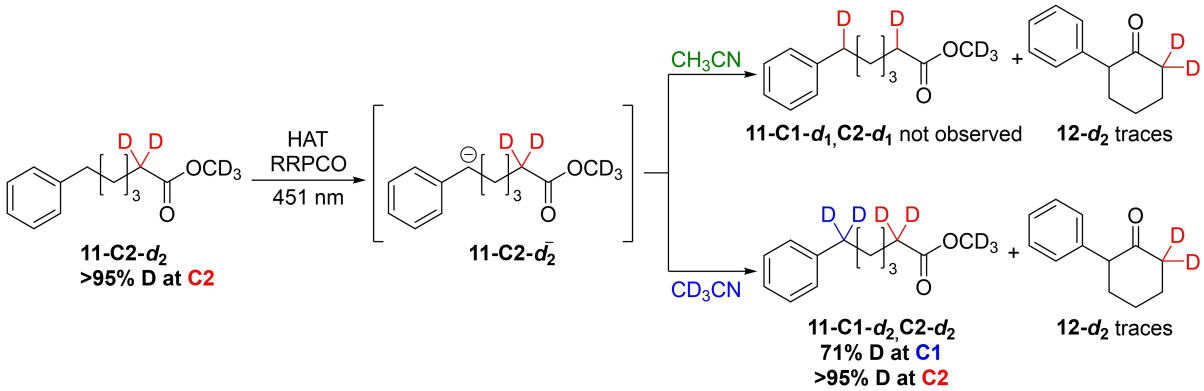


***Scheme 7.*** Carbanion generation at the benzylic position of 6-phenylhexanoic acid ester **11-C2-$d_2$** results only in traces of the corresponding 2-phenylcyclohexanone (**12-$d_2$**) and no intramolecular deuterium-shift. A high degree of deuteration at the benzylic position if $CD_3CN$ is used as solvent confirms benzylic C-H activation to the corresponding carbanion under the reaction conditions.

a 1:1 ratio in near quantitative combined yield. The toluene derivative had a high degree of mono-deuteration (94%) demonstrating that the yield of tertiary alcohol is limited by the competing reactivity of the carbanion acting as base instead of nucleophile, and, thus, factors such as residual moisture or radical side reactions are negligible.

When electron withdrawing groups (EWG) stabilize the carbanion, its nucleophilic reactivity is decreased and lower yield for addition to aldehydes and ketones is observed (Scheme 9). However, basicity of the carbanion **1g**$^-$ is still high enough to deprotonate the α-position of acetone resulting in protonation of the carbanion as the major

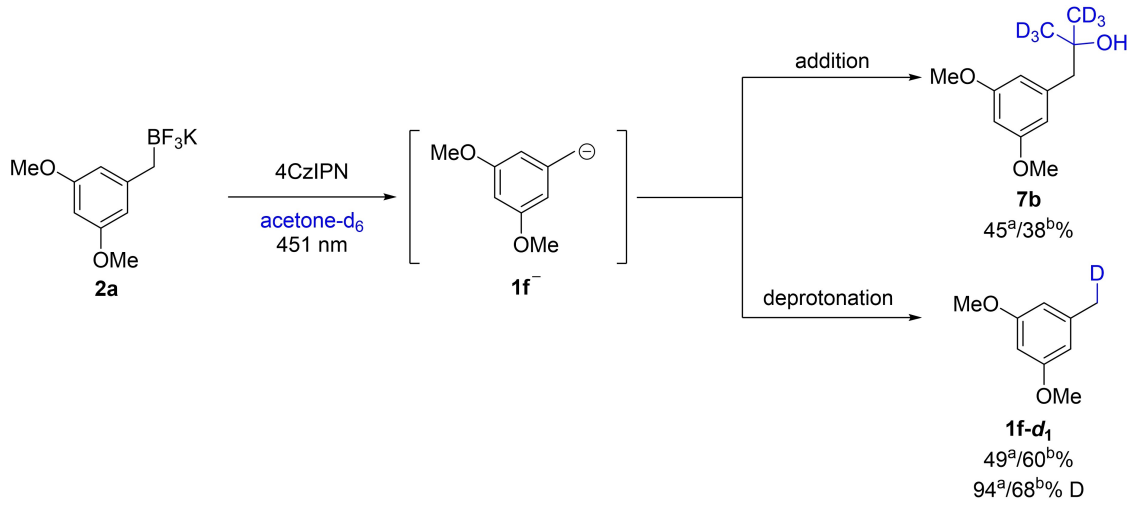


***Scheme 8.*** Benzylic carbanion **1f**$^-$ reacts with acetone in a Grignard-type addition and in a deprotonation. [a]In acetone-$d_6$ as solvent; [b]in 1:1 mixture acetone-$d_6$/acetonitrile-$d_0$; $^i$Pr$_3$SiSH was used as HAT-reagent, 4CzIPN was used as pre-catalyst. The active catalyst was formed in situ via photosubstitution.[22]

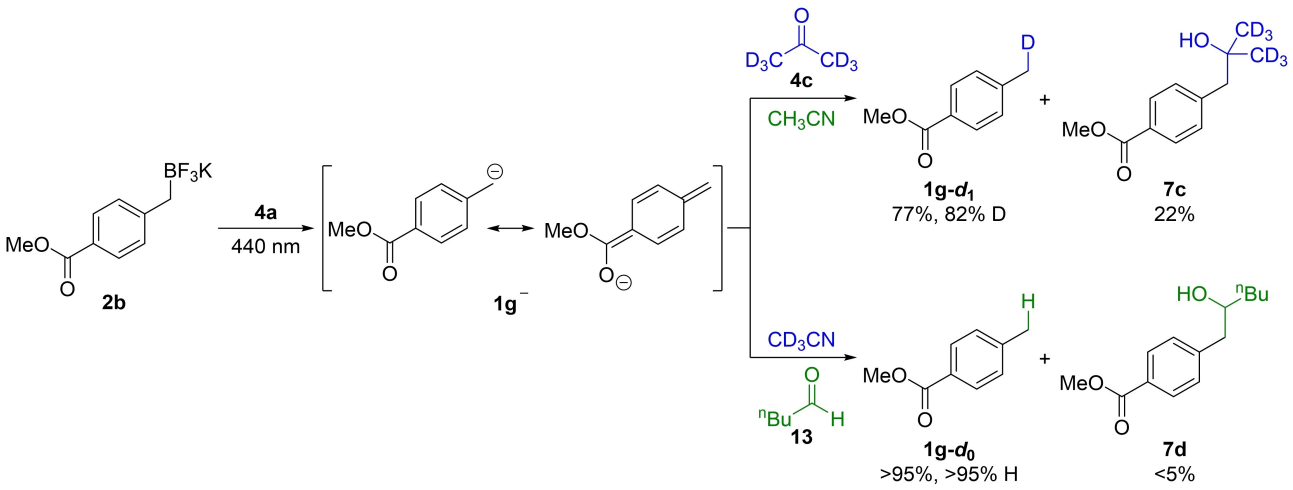


***Scheme 9.*** Stabilization of benzylic carbanions by electron withdrawing groups reduces their nucleophilicity. Despite reduced basicity deprotonation of aldehydes and ketones is still possible, thus giving the corresponding toluene derivative as the major product. Yields and deuteration determined by $^1$H NMR spectroscopy.

reaction pathway. When using the less electrophilic reaction partner ethyl acetate as solvent, no addition product is observed while deprotonation is still the predominant reaction pathway, which was indirectly observed in the $^2$H NMR spectrum in the presence of $D_2O$, showing a signal for mono-deuterated ethyl acetate (see Supporting Information Figure S32). This again demonstrates that reactivity of photocatalytically generated carbanions is predominantly limited by their high basicity.

To note, 4CzIPN itself acts as a photocatalyst only if substrates are substituted with electron withdrawing groups or sterically hindered substrates are used, while primary benzylic radicals substituted with electron donating groups first react in a photosubstitution reaction substituting one of the CN-groups to form the active catalyst.[22] Accordingly, the reduction of electron poor benzyl radicals is favored over radical recombination with the 4CzIPN radical anion while neutral and electron rich benzyl radicals are difficult to reduce by the 4CzIPN radical anion and rather trigger photosubstitution of 4CzIPN (**4b**) forming a more stable and stronger reducing photocatalyst. The observation that electron withdrawing groups lead to favoring RRPCO over other reaction pathways even for only moderately reducing photocatalysts explains previous reports.[35] For instance, the reactivity of benzyltriphenylphosphonium salts (**14**) under reductive photocatalytic conditions strongly depends on the electronic nature of substituents on the aromatic ring. While electron-rich benzyl radicals dimerize to the corresponding bibenzyls, benzyltriphenylphosphonium salts bearing electron withdrawing groups such as **14a** exclusively form the corresponding toluene derivative (substrate **14a** gives toluene derivative **1g**). Due to deuteration of the benzylic

position when $CD_3CN$ was used as solvent a HAT from the solvent acetonitrile or, depending on the electron donor, from an amine radical cation to the benzyl radical was proposed to occur with electron deficient benzyl radicals, while dimerization to the bibenzyl was proposed to be unfavored due to a polarity mismatch. However, this could not explain, for instance, a difference in the product distribution, if started from a benzyl bromide instead of a benzyltriphenylphosphonium salt. Furthermore, the proposed HAT is energetically not plausible, since the bond dissociation energy (BDE) of toluenes (88 kcal/mol for unsubstituted toluene)[36] is below that of acetonitrile (96 kcal/mol).[37]

Based on the results presented in this work, we suggest to revise the mechanism for electron-withdrawing group substituted benzyltriphenylphosphonium salts according to Scheme 10. The iridium-based photocatalyst $[Ir(dtbbpy)(ppy)_2]PF_6$ used is slightly more reducing compared to 4CzIPN (−1.51 V[38] and -1.24 V[31] vs. SCE). For electron rich benzyl radicals reduction to carbanions is slow or not feasible (−1.43 V vs. SCE for unsubstituted benzyl radical in MeCN)[25] so that benzyl radical build-up leads to dimerization as proposed. In contrast, electron-deficient benzyl radicals such as **1g**° are faster reduced to the corresponding carbanions than a critical benzyl radical concentration for dimerization will build up. The carbanion is not able to form bibenzyl, but it is sufficiently basic to deprotonate either the amine radical cation (if DIPEA is used as sacrificial electron donor) or just basic enough to deprotonate the solvent acetonitrile (see Scheme 3) in the absence of more acidic protons. The different product distribution for benzyl bromide substrates is also easily explained by that mechanism: Since electron deficient benzyl bromides are more easily reduced to generate the corresponding radical (−1.29 V vs. SCE in MeCN), benzyl bromides will mainly form benzyl radicals while radicals are first reduced to carbanions when triphenylphosphonium salts are used as radical precursor, changing from radical to carbanionic reactivity depending on the radical source.

## Conclusion

In conclusion, it was demonstrated that carbanions generated via a photocatalytic RRPCO step are superbasic intermediates capable of deprotonating common polar solvents such as acetonitrile, DMSO, and DMF. Their reactivity is comparable to the gas-phase reactivity of isolated carbanions so that these are best described as monomeric, free carbanions, answering the fundamental question about the nature of these often-proposed intermediates. A general mechanism and methods used in this work are depicted in Scheme 11. Moreover, it was demonstrated, that previously unsuccessful nucleophilic addition and substitution reactions were not limited by the nucleophilicity of the carbanions but by their high basicity towards solvents and abstractable protons commonly present in electrophiles. The time-scale of the individual steps was determined by time-resolved spectroscopy and identified the RRPCO step as rate-limiting with a lifetime of 231 µs for the photocatalyst radical anion reducing a benzyl radical to the carbanion. Kinetic isotope effects and selectivity for deprotonations by photocatalytically generated carbanions can act as mechanistic probe to indirectly detect carbanionic intermediates by their specific reactivity. This was demonstrated for carbanion generation from benzylic C-H bonds, supporting the initially proposed mechanism. Further a substrate dependent change in the mechanism for photoreduction of

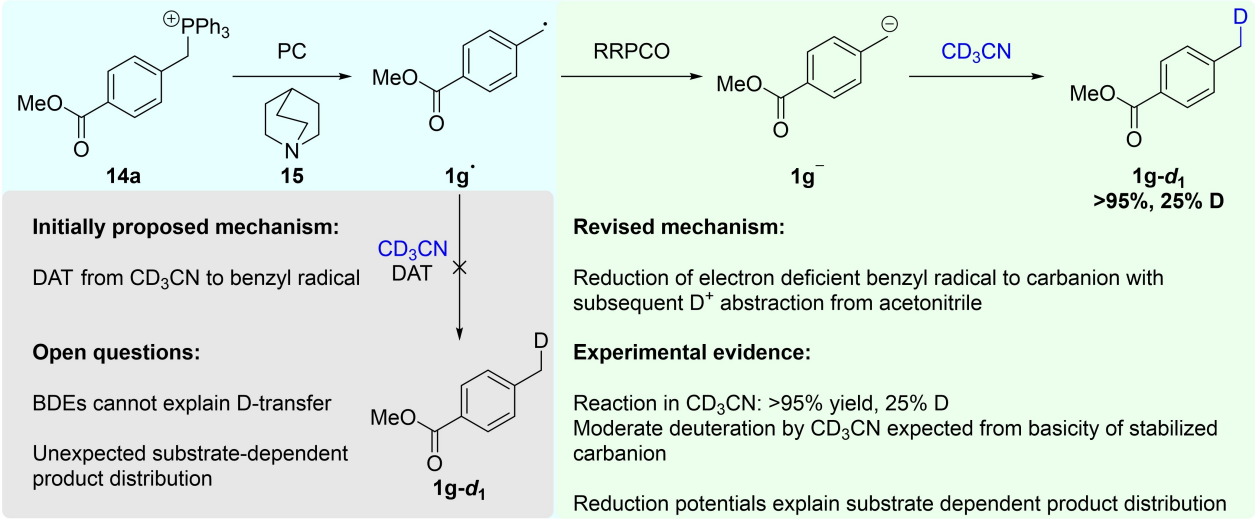


***Scheme 10.*** Electron-withdrawing group substituted benzyltriphenylphosphonium salts undergo reduction to the corresponding toluene derivative, while electron-donating group substituted benzyltriphenylphosphonium salts form bibenzyls under reductive photocatalytic conditions. The initially proposed mechanism[35] via HAT or DAT from acetonitrile is unlikely and instead an RRPCO and subsequent protonation is more plausible as supported by data presented in this work. Abbreviations: BDE—bond dissociation energy, H(D)AT—hydrogen(deuterium) atom transfer, PC—photocatalyst = $[Ir(dtbbpy)(ppy)_2]PF_6$.

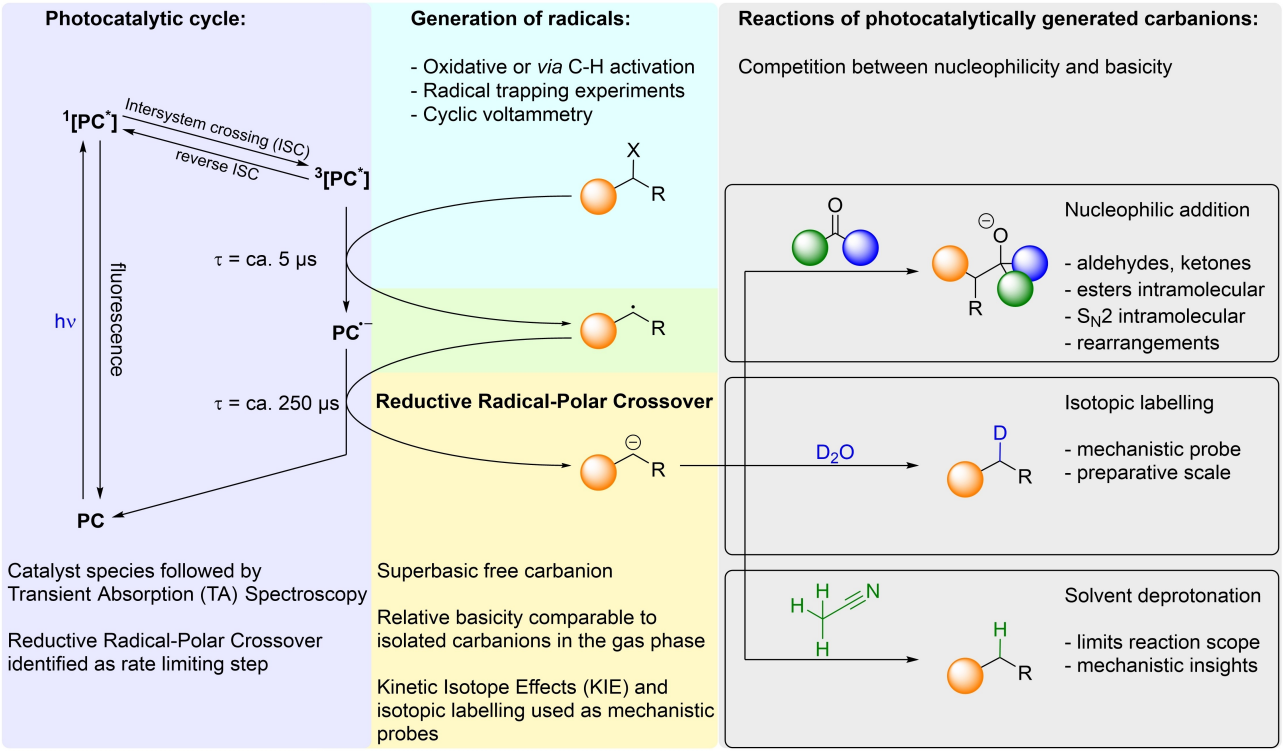


***Scheme 11.*** Summary of the mechanistic cycle for generation of carbanions via photocatalytic reductive radical-polar crossover (RRPCO) and methods used to elucidate the mechanism. Transient species of the photocatalyst (PC) **4d** were followed via transient absorption (TA) spectroscopy with trifluoroborate **2a** as substrate. Decay times should only give an estimate as the bimolecular rate constants are expected to vary depending on the specific substrate, photocatalyst, and concentration. The presence of benzyl radicals was demonstrated in previous work by radical trapping.[9] The reactivity of photocatalytically generated carbanions was investigated with the focus on competing nucleophilicity and basicity. Tandem mass spectrometry was used to compare the basicity in solution to the basicity of isolated carbanions in the gas phase.

benzyltriphenylphosphonium salts was detected. Overall, the results provide an intuitive qualitative estimation of the limits for reactions involving photocatalytically generated carbanions as reactive intermediates and will help to rationally develop solutions to overcome these limitations.

## Supporting Information

The authors have cited additional references within the Supporting Information.[39]

## Acknowledgements

This work was supported by the Deutsche Forschungsgemeinschaft (DFG, German Science Foundation) GRK 2620—426795949 and TRR 325—444632635. We thank Anna Wernsdorfer for support. Open Access funding enabled and organized by Projekt DEAL.

## Conflict of Interest

The authors declare no conflict of interest.

## Data Availability Statement

The data that support the findings of this study are available from the corresponding author upon reasonable request.

**Keywords:** Photocatalysis · Carbanions · Electron transfer · Basicity · Isotope effects

[1] a) K. Donabauer, B. König, *Acc. Chem. Res.* **2021**, *54*, 242; b) L. Pitzer, J. L. Schwarz, F. Glorius, *Chem. Sci.* **2019**, *10*, 8285.
[2] A. L. Berger, K. Donabauer, B. König, *Chem. Sci.* **2019**, *10*, 10991.
[3] K. Donabauer, M. Maity, A. L. Berger, G. S. Huff, S. Crespi, B. König, *Chem. Sci.* **2019**, *10*, 5162.
[4] K. Donabauer, K. Murugesan, U. Rozman, S. Crespi, B. König, *Chemistry* **2020**, *26*, 12945.
[5] V. Babin, A. Talbot, A. Labiche, G. Destro, A. Del Vecchio, C. S. Elmore, F. Taran, A. Sallustrau, D. Audisio, *ACS Catal.* **2021**, *11*, 2968.
[6] R. Abrams, J. Clayden, *Angew. Chem. Int. Ed.* **2020**, *59*, 11600.
[7] T. Xiao, L. Li, L. Zhou, *J. Org. Chem.* **2016**, *81*, 7908.
[8] J. P. Phelan, S. B. Lang, J. S. Compton, C. B. Kelly, R. Dykstra, O. Gutierrez, G. A. Molander, *J. Am. Chem. Soc.* **2018**, *140*, 8037.
[9] Q.-Y. Meng, T. E. Schirmer, A. L. Berger, K. Donabauer, B. König, *J. Am. Chem. Soc.* **2019**, *141*, 11393.

[10] K. Murugesan, K. Donabauer, R. Narobe, V. Derdau, A. Bauer, B. König, *ACS Catal.* **2022**, *12*, 3974.

[11] M. Schmalzbauer, T. D. Svejstrup, F. Fricke, P. Brandt, M. J. Johansson, G. Bergonzini, B. König, *Chem* **2020**, *6*, 2658.

[12] L.-L. Liao, G.-M. Cao, J.-H. Ye, G.-Q. Sun, W.-J. Zhou, Y.-Y. Gui, S.-S. Yan, G. Shen, D.-G. Yu, *J. Am. Chem. Soc.* **2018**, *140*, 17338.

[13] C.-K. Ran, Y.-N. Niu, L. Song, M.-K. Wei, Y.-F. Cao, S.-P. Luo, Y.-M. Yu, L.-L. Liao, D.-G. Yu, *ACS Catal.* **2022**, *12*, 18.

[14] a) J. I. Day, S. Grotjahn, S. Senaweera, B. Koenig, J. D. Weaver, *J. Org. Chem.* **2021**, *86*, 7928; b) A. R. Flynn, K. A. McDaniel, M. E. Hughes, D. B. Vogt, N. T. Jui, *J. Am. Chem. Soc.* **2020**, *142*, 9163; c) R. C. McAtee, E. A. Noten, C. R. J. Stephenson, *Nat. Commun.* **2020**, *11*, 2528; d) J. P. Cole, D.-F. Chen, M. Kudisch, R. M. Pearson, C.-H. Lim, G. M. Miyake, *J. Am. Chem. Soc.* **2020**, *142*, 13573.

[15] a) F. El-Hage, C. Schöll, J. Pospech, *J. Org. Chem.* **2020**, *85*, 13853; b) R. Kleinmans, L. E. Will, J. L. Schwarz, F. Glorius, *Chem. Sci.* **2021**, *12*, 2816.

[16] V. R. Yatham, Y. Shen, R. Martin, *Angew. Chem. Int. Ed.* **2017**, *56*, 10915.

[17] W. Zhang, L. Lu, W. Zhang, Y. Wang, S. D. Ware, J. Mondragon, J. Rein, N. Strotman, D. Lehnherr, K. A. See, et al., *Nature* **2022**, *604*, 292.

[18] D. Seyferth, *Organometallics* **2009**, *28*, 1598.

[19] H. J. Reich, *Chem. Rev.* **2013**, *113*, 7130.

[20] a) D. Kong, M. Munch, Q. Qiqige, C. J. C. Cooze, B. H. Rotstein, R. J. Lundgren, *J. Am. Chem. Soc.* **2021**, *143*, 2200; b) B. Zhang, Y. Yi, Z.-Q. Wu, C. Chen, C. Xi, *Green Chem.* **2020**, *22*, 5961; c) K. Benedetti Vega, J. A. Campos Delgado, L. V. B. L. Pugnal, B. König, J. T. Menezes Correia, M. Weber Paixão, *Chemistry* **2022**, e202203625.

[21] H. Gilman, R. V. Young, *J. Org. Chem.* **1936**, *01*, 315.

[22] S. Grotjahn, B. König, *Org. Lett.* **2021**, *23*, 3146.

[23] W. S. Matthews, J. E. Bares, J. E. Bartmess, F. G. Bordwell, F. J. Cornforth, G. E. Drucker, Z. Margolin, R. J. McCallum, G. J. McCollum, N. R. Vanier, *J. Am. Chem. Soc.* **1975**, *97*, 7006.

[24] S. Kopf, F. Bourriquen, W. Li, H. Neumann, K. Junge, M. Beller, *Chem. Rev.* **2022**, *122*, 6634.

[25] B. A. Sim, D. Griller, D. D. M. Wayner, *J. Am. Chem. Soc.* **1989**, *111*, 754.

[26] X. M. Zhang, F. G. Bordwell, M. van der Puy, H. E. Fried, *J. Org. Chem.* **1993**, *58*, 3060.

[27] F. G. Bordwell, W. J. Boyle, *J. Am. Chem. Soc.* **1971**, *93*, 512.

[28] G. Qiu, C.-L. Ni, R. R. Knowles, *J. Am. Chem. Soc.* **2023**, *145*, 11537.

[29] A. L. Berger, K. Donabauer, B. König, *Chem. Sci.* **2018**, *9*, 7230.

[30] T. J. Curphey, L. D. Trivedi, T. Layloff, *J. Org. Chem.* **1974**, *39*, 3831.

[31] E. Speckmeier, T. G. Fischer, K. Zeitler, *J. Am. Chem. Soc.* **2018**, *140*, 15353.

[32] C. Franco, J. Olmsted, *Talanta* **1990**, *37*, 905.

[33] R.-J. Kutta, T. Langenbacher, U. Kensy, B. Dick, *Appl. Phys. B* **2013**, *111*, 203.

[34] X. Duan, S. Scheiner, *J. Am. Chem. Soc.* **1992**, *114*, 5849.

[35] A. M. Boldt, S. I. Dickinson, J. R. Ramirez, A. M. Benz-Weeden, D. S. Wilson, S. M. Stevenson, *Org. Biomol. Chem.* **2021**, *19*, 7810.

[36] S. L. Khursan, D. A. Mikhailov, V. M. Yanborisov, D. I. Borisov, *React. Kinet. Catal. Lett.* **1997**, *61*, 91.

[37] Y.-R. Luo, *Handbook of bond dissociation energies in organic compounds*, CRC Press, Boca Raton, Fla. **2003**.

[38] M. S. Lowry, J. I. Goldsmith, J. D. Slinker, R. Rohl, R. A. Pascal, G. G. Malliaras, S. Bernhard, *Chem. Mater.* **2005**, *17*, 5712.

[39] a) E. Andris, J. Jašík, L. Gómez, M. Costas, J. Roithová, *Angew. Chem. Int. Ed.* **2016**, *55*, 3637; b) N. Archipowa, R. J. Kutta, D. J. Heyes, N. S. Scrutton, *Angew. Chem. Int. Ed.* **2018**, *57*, 2682; c) P. B. Armentrout, *J. Am. Soc. Mass Spectrom.* **2002**, *13*, 419; d) P. Armentrout, *Int. J. Mass Spectrom.* **2000**, *200*, 219; e) R. C. Binning, L. A. Curtiss, *J. Comput. Chem.* **1990**, *11*, 1206; f) J.-P. Blaudeau, M. P. McGrath, L. A. Curtiss, L. Radom, *J. Chem. Phys.* **1997**, *107*, 5016; g) J.-D. Chai, M. Head-Gordon, *Phys. Chem. Chem. Phys.* **2008**, *10*, 6615; h) K. C. Crellin, E. Sible, J. van Antwerp, *Int. J. Mass Spectrom.* **2003**, *222*, 281; i) Z. Deng, S. Han, M. Ke, Y. Ning, F.-E. Chen, *Chem. Commun.* **2022**, *58*, 3921; j) B. Dick, U. Kensy, R. J. Kutta in *Chemical Photocatalysis* (Ed.: B. König), De Gruyter, Berlin, Boston **2020**, pp. 415–442; k) S. Engle, T. R. Kirkner, C. B. Kelly, *Org. Synth.* **2019**, *96*, 455; l) M. Espinal-Viguri, S. E. Neale, N. T. Coles, S. A. Macgregor, R. L. Webster, *J. Am. Chem. Soc.* **2019**, *141*, 572; m) E. M. Espinoza, J. A. Clark, J. Soliman, J. B. Derr, M. Morales, V. I. Vullev, *J. Electrochem. Soc.* **2019**, *166*, H3175–H3187; n) M. M. Francl, W. J. Pietro, W. J. Hehre, J. S. Binkley, M. S. Gordon, D. J. DeFrees, J. A. Pople, *J. Chem. Phys.* **1982**, *77*, 3654; o) M. S. Gordon, *Chem. Phys. Lett.* **1980**, *76*, 163; p) J. W. Greenwood, B. T. Boyle, A. McNally, *Chem. Sci.* **2021**, *12*, 10538; q) S. Grimme, *J. Comput. Chem.* **2006**, *27*, 1787; r) S. Grimme, S. Ehrlich, L. Goerigk, *J. Comput. Chem.* **2011**, *32*, 1456; s) P. C. Hariharan, J. A. Pople, *Theor. Chim. Acta* **1973**, *28*, 213; t) T. Hartman, M. Reisnerová, J. Chudoba, E. Svobodová, N. Archipowa, R. J. Kutta, R. Cibulka, *ChemPlusChem* **2021**, *86*, 373; u) T. Hashimoto, T. Ishimaru, K. Shiota, Y. Yamaguchi, *Chem. Commun.* **2020**, *56*, 11701; v) W. J. Hehre, W. A. Lathan, *J. Chem. Phys.* **1972**, *56*, 5255; w) L. Jašíková, J. Roithová, *Organometallics* **2012**, *31*, 1935; x) N. R. M. de Kler, J. Roithová, *Chem. Commun.* **2020**, *56*, 12721; y) R. J. Kutta, *PhD Thesis*, University of Regensburg, Regensburg, **2012**; z) R. J. Kutta, N. Archipowa, N. S. Scrutton, *Phys. Chem. Chem. Phys.* **2018**, *20*, 28767; aa) J. Luo, B. Hu, W. Wu, M. Hu, T. L. Liu, *Angew. Chem. Int. Ed.* **2021**, *60*, 6107; ab) P. Marquet, N. Venisse, É. Lacassie, G. Lachâtre, *Analusis* **2000**, *28*, 925; ac) K. Motoshima, M. Ishikawa, Y. Hashimoto, K. Sugita, *Bioorg. Med. Chem.* **2011**, *19*, 3156; ad) S. Nomura, K. Endo-Umeda, A. Aoyama, M. Makishima, Y. Hashimoto, M. Ishikawa, *ACS Med. Chem. Lett.* **2015**, *6*, 902; ae) J. F. Parcher, M. Wang, A. G. Chittiboyina, I. A. Khan, *Drug Test Anal.* **2018**, *10*, 28; af) G. A. Petersson, M. A. Al-Laham, *J. Chem. Phys.* **1991**, *94*, 6081; ag) V. A. Rassolov, J. A. Pople, M. A. Ratner, T. L. Windus, *J. Chem. Phys.* **1998**, *109*, 1223; ah) V. A. Rassolov, M. A. Ratner, J. A. Pople, P. C. Redfern, L. A. Curtiss, *J. Comput. Chem.* **2001**, *22*, 976; ai) P. K. Sahoo, Y. Zhang, Y. Qin, P. Ren, R. Cauwenbergh, G. Siva Raman, S. Das, *J. Catal.* **2023**, *425*, 80; aj) B. Siegel, *J. Am. Chem. Soc.* **1979**, *101*, 2265; ak) E. E. Stache, T. Rovis, A. G. Doyle, *Angew. Chem. Int. Ed.* **2017**, *56*, 3679; al) E. Teloy, D. Gerlich, *Chem. Phys.* **1974**, *4*, 417; am) F. Wakayama, R. Ito, K. Park, M. Ishida, Y. Yamada, S. Ichihara, H. Takada, S. Nakamura, A. Kato, T. Yamada, et al., *Bull. Chem. Soc. Jpn.* **2021**, *94*, 2702; an) D. D. M. Wayner, D. J. McPhee, D. Griller, *J. Am. Chem. Soc.* **1988**, *110*, 132; ao) F. Weigend, *Phys. Chem. Chem. Phys.* **2006**, *8*, 1057; ap) F. Weigend, R. Ahlrichs, *Phys. Chem. Chem. Phys.* **2005**, *7*, 3297; aq) W.-Z. Weng, H. Liang, B. Zhang, *Org. Lett.* **2018**, *20*, 4979; ar) X.-B. Yan, C.-L. Li, W.-J. Jin, P. Guo, X.-Z. Shu, *Chem. Sci.* **2018**, *9*, 4529; as) M. J. Frisch, G. W. Trucks, H. B. Schlegel, G. E. Scuseria, M. A. Robb, J. R. Cheeseman, G. Scalmani, V. Barone, G. A. Petersson, H. Nakatsuji, X. Li, M. Caricato, A. V. Marenich, J. Bloino, B. G. Janesko, R. Gomperts, B. Mennucci, H. P. Hratchian, J. V. Ortiz, A. F. Izmaylov, J. L. Sonnenberg, D. Williams-Young, F. Ding, F. Lipparini, F. Egidi, J. Goings, B.

Peng, A. Petrone, T. Henderson, D. Ranasinghe, V. G. Zakrzewski, J. Gao, N. Rega, G. Zheng, W. Liang, M. Hada, M. Ehara, K. Toyota, R. Fukuda, J. Hasegawa, M. Ishida, T. Nakajima, Y. Honda, O. Kitao, H. Nakai, T. Vreven, K. Throssell, J. A. Montgomery, Jr., J. E. Peralta, F. Ogliaro, M. J. Bearpark, J. J. Heyd, E. N. Brothers, K. N. Kudin, V. N. Staroverov, T. A. Keith, R. Kobayashi, J. Normand, K. Raghavachari, A. P. Rendell, J. C. Burant, S. S. Iyengar, J. Tomasi, M. Cossi, J. M. Millam, M. Klene, C. Adamo, R. Cammi, J. W. Ochterski, R. L. Martin, K. Morokuma, O. Farkas, J. B. Foresman, D. J. Fox, *Gaussian 16, Revision C.01*, Gaussian, Inc., Wallingford CT **2019**.

Manuscript received: January 12, 2024
Accepted manuscript online: February 26, 2024
Version of record online: March 15, 2024